Technical Note: DIRART – A software suite for deformable image registration and adaptive radiotherapy research

Deshan Yang,[a] Scott Brame, Issam El Naqa, Apte Aditya, Yu Wu, S. Murty Goddu, Sasa Mutic, Joseph O. Deasy, and Daniel A. Low
Department of Radiation Oncology, School of Medicine, Washington University in Saint Louis, Missouri 63110

(Received 2 September 2010; revised 27 October 2010; accepted for publication 8 November 2010; published 14 December 2010)

Purpose: Recent years have witnessed tremendous progress in image guide radiotherapy technology and a growing interest in the possibilities for adapting treatment planning and delivery over the course of treatment. One obstacle faced by the research community has been the lack of a comprehensive open-source software toolkit dedicated for adaptive radiotherapy (ART). To address this need, the authors have developed a software suite called the Deformable Image Registration and Adaptive Radiotherapy Toolkit (DIRART).
Methods: DIRART is an open-source toolkit developed in MATLAB. It is designed in an object-oriented style with focus on user-friendliness, features, and flexibility. It contains four classes of DIR algorithms, including the newer inverse consistency algorithms to provide consistent displacement vector field in both directions. It also contains common ART functions, an integrated graphical user interface, a variety of visualization and image-processing features, dose metric analysis functions, and interface routines. These interface routines make DIRART a powerful complement to the Computational Environment for Radiotherapy Research (CERR) and popular image-processing toolkits such as ITK.
Results: DIRART provides a set of image processing/registration algorithms and postprocessing functions to facilitate the development and testing of DIR algorithms. It also offers a good amount of options for DIR results visualization, evaluation, and validation.
Conclusions: By exchanging data with treatment planning systems via DICOM-RT files and CERR, and by bringing image registration algorithms closer to radiotherapy applications, DIRART is potentially a convenient and flexible platform that may facilitate ART and DIR research. © *2011 American Association of Physicists in Medicine*. [DOI: 10.1118/1.3521468]

Key words: adaptive radiotherapy, image registration, voxel mapping, image segmentation, deformation, image processing, MATLAB, open source, CERR

I. INTRODUCTION

Adaptive radiotherapy (ART) has been a salient research topic for more than a decade.[1] Research on ART can benefit from software toolkits that facilitate efficient sharing of data and rapid development and distribution of relevant tools. In the case of IMRT, this need was addressed by the Computational Environment for Radiotherapy Research (CERR),[2] an open-source toolkit developed using MATLAB. By most measures, CERR has been a tremendous success, having been downloaded more than 3000 times and used in support of 60+ peer-reviewed publications and countless research projects. In this article, we describe an elaboration on, or accompaniment to, CERR, known as the Deformable Image Registration and Adaptive Radiotherapy Research Toolbox (DIRART) that has been developed to meet the unique needs of ART and DIR research.

The central idea behind ART is that adaptation of a treatment plan over the course of treatment can, in some instances, result in better therapeutic ratios than those that would have resulted from delivery of the original treatment plan. Plans are, and have been, adapted for patients for many years, typically in response to weight loss or other "significant" morphological changes. What differentiates ART is not the adaptation of plans, but rather the framework for deciding that plans need to be adapted and the manner in which they are adapted (e.g., accept/reject regions, dose accumulation, etc.). In this way, ART is similar to image guided radiotherapy (IGRT):[3–5] IGRT refers not to the use of images to guide radiotherapy, something we have done for many years, but rather to a normative framework for extracting and acting upon information contained within images (e.g., no-action level positioning protocol,[6,7] shrinking-action level protocol,[8,9] etc.).

Broadly speaking, the proposed approaches to ART rely on metrics of three basic types: geometric,[1,8,10] dosimetric,[11] and functional.[12,13] Research on these metrics is entangled, with deformable registration[14–16] and autosegmentation[17,18] being common threads. For example, calculating an accumulated dose requires voxel mapping between fractions and calculation of single-fraction DVHs requires reliable autosegmentation of in-room imagery.[19–21] In terms of plan adaptation, one may consider that the problem lies in doing what has always been done, just with different inputs and much more quickly. Under some ART schemes, there is a

need for injecting coverage probabilities into the optimization of IMRT plans,[1,22] in others the need for quick and accurate application of a plan to a new image set.[8,23] Clearly, image segmentation/registration and optimization[24,25]/replanning[8,23] will continue to occupy ART researchers for years to come.

With this view of the needs of ART, it is clear that a robust research toolkit would include broad support for segmentation/registration research as well as a full complement of more traditional IMRT and planning research. CERR continues to evolve in such a manner as to suffice for the second, and tools, such as ITK,[26] VTK,[27] and MITK,[28] have demonstrated their utility in the imaging community. What we describe in this article, DIRART, aims to bridge the gaps between such systems and provides the foundation for a comprehensive ART research toolkit. It is open-source, based on MATLAB, designed for easy connection with ITK algorithms and CERR, and, as we shall show, has a variety of unique functions and features that can aid ART research.

The goal of DIRART is not to supplant existing commercial or research packages, but to provide a complement that can grow and evolve under the influence of open-source collaboration and development. In what follows, we will introduce the high-level design concepts underlying DIRART, provide an overview of basic functions, tools, and views, and then give an example of how DIRART is being used in our research. The article concludes with a discussion of computation speed, software distribution and licensing, and plans for future DIRART development.

II. METHOD AND MATERIALS

II.A. Overview

DIRART was started in 2007 as a deformable image registration program built on top of a simple graphical user interface (GUI). In the interim, DIRART has undergone several major revisions and currently consists of 450+ MATLAB program files (with 40 000+ lines of code), and a large number of C/C++ programs that enable easy interfacing with non-MATLAB packages (such as ITK). DIRART uses CERR functions for DICOM import and export, so users should install DIRART alongside CERR. Except for import/export, it runs independently of CERR, thus allowing users full access to all major functions, visualization features and configuration options through the DIRART user interface. DIRART functions can also be invoked from external MATLAB programs, which allow routine DIR and ART tasks to be initiated and ran without direct user interaction.

As shown in Fig. 1, DIRART has two main functional components, one for image registration and one for ART, as well as supporting components for data input/export and a common visualization environment. The image registration and ART components are linked by voxel mapping, which is the result of DIR and the critical piece for ART data processing. Voxel mapping describes how the tissues deform and relocate between the different image sets of the same patient, or in other words, tells how the misaligned patient data can be realigned.

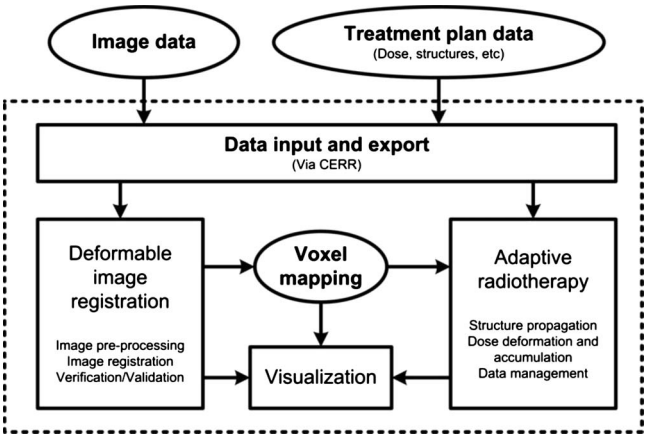

FIG. 1. DIRART functional components and general workflow. The blocks are the functional components. The ovals are the data. The arrows represent the data flow. The dashed line encloses DIRART components and data.

From a users' standpoint, DIRART can be (1) a collection of DIR algorithms; (2) a MATLAB ART toolbox that can perform dose and structure remapping, dose accumulation, and analysis; (3) a treatment plan viewer with many visualization options; (4) a viewer and verification tool for DIR results; and (5) a complementary package to CERR that offers additional image registration and ART functions. Moreover, by exchanging DICOM-RT data, it could be used an external software tool, in conjunction with commercial treatment planning systems.

II.B. Design of DIRART

As illustrated in Fig. 2, DIRART is designed around the concept of individual and interactive RT data objects. Examples of RT objects that DIRART currently handles include images, structures, doses, and deformation vector fields (DVFs).

All RT objects are processed in DIRART independently based on their physical representations (voxel coordinates, voxel sizes, origin, orientation, etc.). For example, a structure object contains a collection of contour points that share the same coordinate system as the associated image. However, the deformed structure is independent of the CT images because its contour points are not necessarily on the CT slices (i.e., association has been broken). A dose volume shares the same physical coordinate system as the CT scans and structures, but could have a different volumetric coverage and voxel sizes. By allowing such independence, DIRART allows researchers to quickly transform RT objects between different representations and volumes, or move them between different physical coordinate systems. For example, image registration could be performed on cropped image volumes with user-selected spatial resolutions. The resulting DVF, which is defined only on the cropped image volume, can then be applied to the original CT scans (before cropping and with different spatial resolutions) or to the structures in support of various ART tasks.

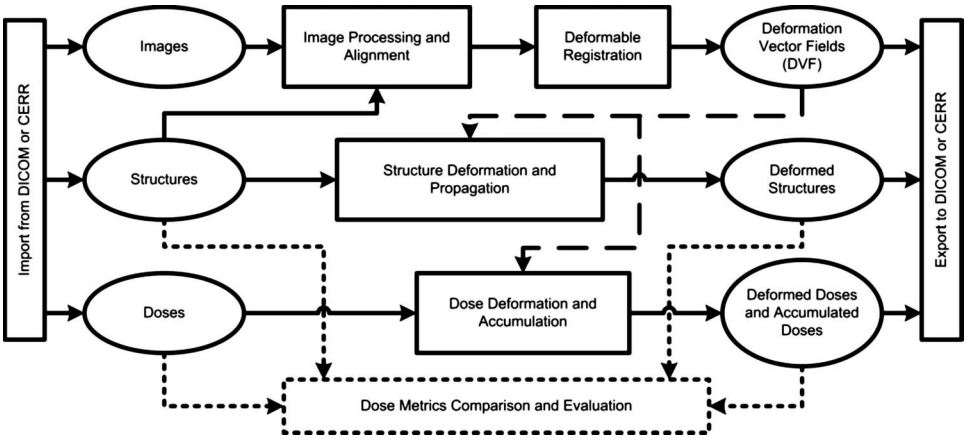

FIG. 2. DIRART is designed around the concepts of RT objects, including images, structures, doses, and DVFs. These RT objects (in ovals) interact via different DIR and ART tasks (in rectangles). The dashed arrows emphasize how DVFs (or voxel mapping) are applied to remap structures and doses. The dotted arrows emphasize that DIRART calls external CERR functions to do dose metric operations (DVHs, etc.).

II.C. Data import and export

II.C.1. Data import

DIRART can directly import images and other radiotherapy data in DICOM files by using the functions in CERR (Ref. 2) and the MATLAB DICOM toolbox. It can also import CERR plan files if users have already saved the image and plan data in CERR format. DIRART can use image data in MATLAB matrix format for general image process and registration practices.

II.C.2. Data saving, reloading, and exporting

DIRART stores its internal data as a multiple level MATLAB structure. The user may save this data structure (as a MATLAB .mat file) and later load it back. This data format also allows DIRART's internal data to be exported to the MATLAB working environment so that it can be further processed using other MATLAB programs and functions.

To communicate with other software packages, DIRART can insert the generated data (deformed images, remapped or accumulated dose volumes, and remapped structures) into the CERR plans from which the original data were imported. It can also export such data directly to DICOM files by using CERR and MATLAB DICOM functions.

II.D. The image registration component

Figure 3 shows the image registration workflow in DIRART that contains image processing, image alignment, deformable image registration, and results evaluation.

II.D.1. Image processing

DIRART contains a number of common image-processing tools. Examples of those that are useful for DIR include the following: (1) Image smoothing (Gaussian low pass smoothing and ten different edge preserving smoothing filters[29]), (2) histogram equalization (regular and contrast limited[30]), (3) window level transformation, (4) KVCT to MVCT intensity remapping,[14] (5) detection and segmentation of bowel gas pockets,[14] (6) image resampling filters, (7) image cropping, (8) image padding (allows registration between images with different volumetric coverages[31]), (9) image intensity manipulation on a per structure basis (allows structural information to be utilized in the DIR computation[14]), and (10) mathematical operators that may be applied to image intensity arrays/values. Most of these image-processing tools were developed for DIRART. A few image smoothing and histogram equalization tools were based on existing MATLAB functions or other existing software packages. The open-source architecture of DIRART and its interfaces with MATLAB, CERR, and external systems, such as ITK, make it relatively simple for researchers to deploy additional image-processing tools.

II.D.2. Rigid image registration/alignment

DIRART imports rigid image registration results (as transformation matrices) directly from CERR and DICOM-RT files. DIRART supports interest point-based and manual registration. The former allows the user to select interest points (e.g., beam isocenters) that are used to determine the registration.

II.D.3. Deformable image registration in DIRART

Image registration computes voxel mapping between two image sets. It is usually formulated as an optimization problem. The solution, i.e., the voxel mapping, is found by maximizing the similarity between the two images, where "simi-

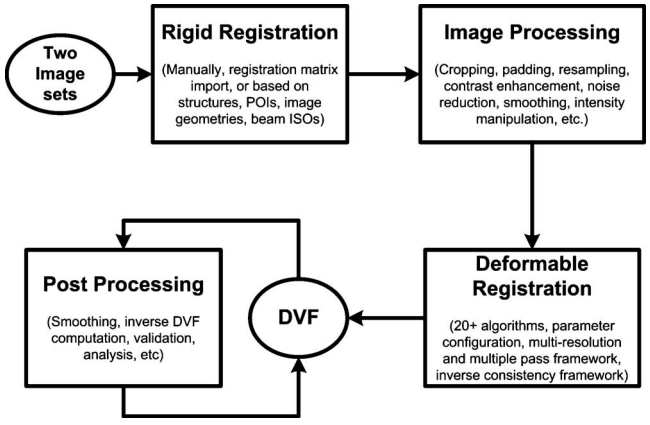

FIG. 3. The general workflow of image processing and registration in DIRART.

TABLE I. List of deformable image registration algorithms in DIRART.

Class	Variations
Optical flow algorithms	HS (Horn–Schunck) algorithm[a] (5 variations) LK (Lucas–Kanade) algorithm[b] (2 variations) HS and LK Combined algorithm[c] Iterative optical flow algorithm (5 variations)[d]
Demons algorithms	Thirion's original demons algorithm[e] Accelerated demons algorithm[f] Symmetric force demons algorithm[g] and other minor 3 variations
Level-set algorithms	Original level-set algorithm[h] and 3 other minor variations
B-spline algorithm	Implemented in ITK and linked into DIRART

[a]Reference 38.
[b]Reference 39.
[c]Reference 40.
[d]References 41 and 42.
[e]Reference 37.
[f]Reference 43.
[g]Reference 44.
[h]Reference 45.

larity" is defined with respect to a figure of merit such as mutual information. Image registration algorithms can be grouped into rigid and deformable (i.e., nonrigid) registrations.[32] Rigid registration typically refers to affine transformations that make use of $\leq$12 free parameters; DIR, on the other hand, makes use of a much larger number of free parameters, enabling, in principle, researchers to capture the dynamics of soft tissue shape changes.

Two common DIR frameworks are implemented in DIRART: (1) The asymmetric registration framework and (2) the inverse consistency registration framework.[33] The asymmetric registration framework deforms one image onto another, producing a "backward DVF." The inverse consistency framework[33] registers both images toward the middle and generates both the forward DVF and backward DVF simultaneously without invoking an explicit DVF inversion as a postoperation. The inverse consistency framework is potentially more accurate but slightly slower. It is particularly relevant for ART applications because both the forward and backward DVFs may be used.

These frameworks support multiresolution[34] (to sequentially register the two images from the lower resolutions to the higher resolutions) and multiple pass[35] approaches. Necessary image resampling,[36] DVF resampling, DVF concatenation, and optional smoothing[37] operations are carried out by the frameworks. The GUI is constantly updated during the DIR computation to display the progresses of the DIR.

Individual DIR algorithms are called by the two frameworks as subroutines. We have implemented a list of image intensity based DIR algorithms in DIRART. DIR algorithms are in three classes: (1) Optical flow algorithms, demons algorithms, and level-set algorithms. Multiple variations are implemented for each class, as listed in Table I. In addition, we have also implemented a common DLL (dynamic-linked library) interface to ITK so that ITK DIR algorithms can be called from DIRART. Currently, five ITK DIR algorithms are supported, including demons algorithms and B-spline algorithms. Updated and new ITK DIR algorithms will be supported in the future.

DIRART offers the following postregistration operations on DVF after a DVF is computed: (1) Smoothing, (2) inverting the DVF (computing the forward DVF from the backward DVF and vice versa), (3) accuracy validation (with a ground truth DVF or landmark pairs), and (4) analysis (Jacobian, magnitude histogram, etc.). DIR validation will be discussed further in Sec. II G.

II.E. The adaptive radiotherapy component

II.E.1. Data remapping

DIRART could transform information (image data, structures, and dose) between the two data sets so that information originally associated with one image could be processed (visualized, evaluated, etc.) on the other image data set. Transformation could be a coordinate value shifting (without deformation) and a DVF based coordinate remapping (with deformation).

Remapping of doses and images is accomplished by resampling the volumetric data. It is technically easier after both forward DVF and backward DVF are computed. Remapping information defined on the moving image onto the fixed image domain needs to use the (regular) backward DVF. Remapping information in the other direction needs to use the forward DVF.

Remapping structures is less straightforward and worth further explanation. Figure 4 shows the workflow of remapping the structures defined on the moving image onto the fixed image. A structure imported from DICOM-RT is as a collection of contour points defined on the 2D slices of the moving image. After these contour points are remapped onto the fixed image, the points are often no longer on the slices of the fixed image. We therefore need to process the remapped structure data (into contour points defined on the slices of the fixed image) before the newly generated struc-

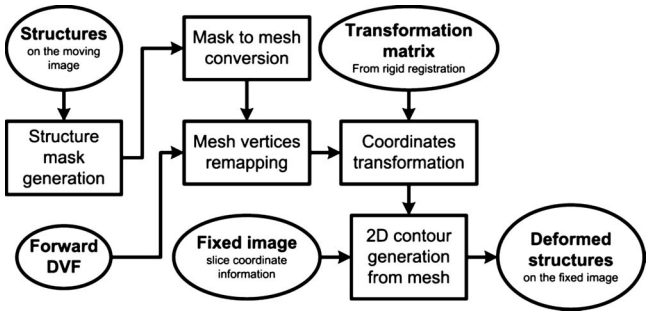

FIG. 4. DIRART structure propagation workflow. This procedure deforms the moving image structures onto the fixed image by using the forward DVF. Data are in ovals and data processing steps are in rectangles.

ture data can be sent back to CERR and exported to DICOM-RT files.

The procedure to remap structures from the fixed image to the moving image is similar to Fig. 4, but the backward DVF is used instead of the forward DVF. Alternatively, structure remapping could be accomplished by deforming the structure mask and then converting the deformed mask volume into 2D contour points. This alternative workflow is also supported by DIRART.

Users can export the remapped data (doses and structures) to CERR and use CERR to perform operations such as DVH computation using deformed doses and structures, or comparison of the deformed or accumulated isodose distributions to the original planned dose distributions using various dose metrics.

II.E.2. Data management

DIRART has a dose manager and a structure manager to control the original and the generated (deformed or remapped) doses and structure objects. The dose manager can load, delete, rescale, add/subtract, and rename doses. Dose subtraction and summation are useful to evaluate the dose difference between fractions and to compute accumulated doses. Both subtraction and summation are performed in conjunction with resampling if doses are in different voxel positions and/or resolutions. The structure manager can rename, shrink, expand, smooth, transfer and delete structures, and control the display of the structures (on/off, line colors, or color wash options). Users can convert the isodose contours into structures and further process (transfer, smooth, export, etc.) them as regular structures.

II.F. Visualization and user interface

DIRART provides a rich set of visualization features with an integrated graphic user interface. DIRART displays all RT objects together in multiple individually configurable viewing panels. Compared to CERR, it has many different visualization options, especially for structures and doses. See Tables II and III for a detailed explanation of available visualization features and options. All configurable options can be accessed via the main GUI window menus, via the context sensitive menu that rises at mouse right button clicking, or by shortcut key combinations.

II.G. Testing and verification

We have performed verification and evaluation (evaluation=indirect verification with lesser accuracy) works for DIRART. However, these works are not expected to be as rigorous as quality assurance required for clinical use. In fact, it is impractical for the authors to test and verify the entire DIRART software package (included DIR algorithms) for all possibilities. It is even impractical to discuss all the

TABLE II. Visualization options for RT objects.

Object	Visualization options
Image	(1) The original images, (2) the difference images (before or after registration), (3) the deformed images, (4) images in composite color channels, (5) checkerboard images (before and after registration), in gray or in color, with and without grid lines, with configurable grid sizes
Dose	(1) Isodose lines (absolute or percent doses), with labels on or off, with or without color filled between lines, (2) dose color wash, (3) both
Structure	**Image association**: (1) Only with associated image, (2) on any image (automatic coordinate transformation)
	Color: User can select color for every individual structure. **Display mode**: (1) In contours, (2) color filled, (3) both
DVF	**DVF to display**: (1) Backward DVF, (2) forward DVF, (3) per-iteration delta DVF, (4) per-pass delta DVF, (5) per-stage (multiresolution stage) delta DVF. **Vector display mode**: (1) Arrows, (2) deformation grids
	DVF scalar data display in color wash: (1) Projection in L-R, (2) in A-P, (3) in S-I, (4) magnitude, (5) Jacobian

TABLE III. General GUI options.

Options	Possible choices
Color map	User can select different color maps for color wash displays options, for dose, image, structures, and DVF
Window levels	Images can be displayed in user-selected window levels, or one of the 6 predefined window level settings
Display panels	Up to 7 individual display panels are supported. Each panel can be individually configured. 5 predefined display layouts are available: 7 small panels, 1 larger+3 small, and so on. Image position (to be displayed) can be locked or unlocked between different display panels
Other display options	(1) Draw image boundary box, (2) draw NaN value boundaries, (3) aspect ratio, (4) display landmarks for registration validation purpose, (5) configurable font sizes, line thickness, transparency.
Mouse actions	(1) Windows level adjustment, (2) zoom in/out, (3) panning, (4) slice changing, (5) reading image intensity values, (6) active display panel selection, (7) position localization cross display panels, etc.

related works (have been done, should be done, and will be done) because of the scope of this article. DIRART is currently a research system only and is not appropriate for clinical use.

II.G.1. Verification of DIR algorithms

Most DIR algorithms in DIRART are implementations of the established algorithms from published literature. They are all verified in their original publications. There are also a few DIR algorithms originally proposed by the authors of this article. For example, the authors proposed a method of using not-a-number (NaN) values to extend the image volumes in order to register two images with mismatching volumes or contents.[31] This method was verified with landmarks for lung CT images and achieved a registration accuracy of 0.8 ± 0.3 mm. The authors also proposed the fast inverse consistency algorithm.[33] It was verified on four image data sets and was shown to be potentially more accurate than the inversely inconsistent counterparts. It must be emphasized that all DIR algorithms were only verified against specific testing data sets in their original publications. The accuracy could vary in great degrees when the same algorithms are applied to different image data sets. The values of the user configurable parameters are also very important.

We have tested the implemented DIR algorithms using our standard image data sets. Our data sets include lung CT images with manually selected landmarks, artificially deformed liver CT images with known DVF, prostate CT images with implanted seeds and structure contours, H/N CT images with manually drawn structure contours, etc. Each DIR algorithms is tested that (1) it basically works, (2) the accuracy is reasonably comparable to other algorithms, (3) the results are reasonably accurate by visual checking, and (4) computation speed is reasonable. DIRART supports two ways to verify the DIR algorithms: (1) Landmark based verification, with manually selected landmark coordinates and (2) ground truth verification, using digital phantoms with ground truth DVF.

There are a few important facts that we have learned from our own verification testing: (1) The DIR algorithms in DIRART only work well on CT images because the algorithms are all based on image intensity matching. (2) CBCT and MVCT images often have intensity slightly different from regular kVCT images. In order to obtain better accuracy, image intensity remapping and window level intensity transformation (both available in DIRART) are often required to preprocess these images before they are registered to regular kVCT image. (3) The B-spline algorithm from ITK could theoretically work on multiple modality images, for instance, CT to MRI, or MRI to MRI, but it has not been fully tested in DIRART. (4) The Horn–Schunck algorithm[38] works best for lung (3D or 4D CT) and head-and-neck (CT to CT, or CT to CBCT) images. Absolute registration accuracy could be around 0.5–1.5 mm.[31] (5) Demons algorithms generally work better for liver, abdomen, and pelvis CT images because of different DVF smoothing methods used in these algorithms. Registration accuracy is usually in the range of 2–20 mm, less than accuracy obtained on lung images. Low soft tissue contrast in these images is the primary reason for lower accuracy. (6) DIR algorithms linked from ITK into DIRART are not tested as thoroughly as algorithms implemented in DIRART. (7) The registration results are usually required to check visually. Users often need to adjust the registration parameters in order to obtain better accuracy.

Complete validation of deformable image registration is a very difficult topic beyond the coverage of this article. It probably deserves more attention by the research community than developing any new DIR algorithms. Unfortunately, there is currently no way to directly validate the deformable image registration results on real patient data sets.

The authors are currently working on a new verification

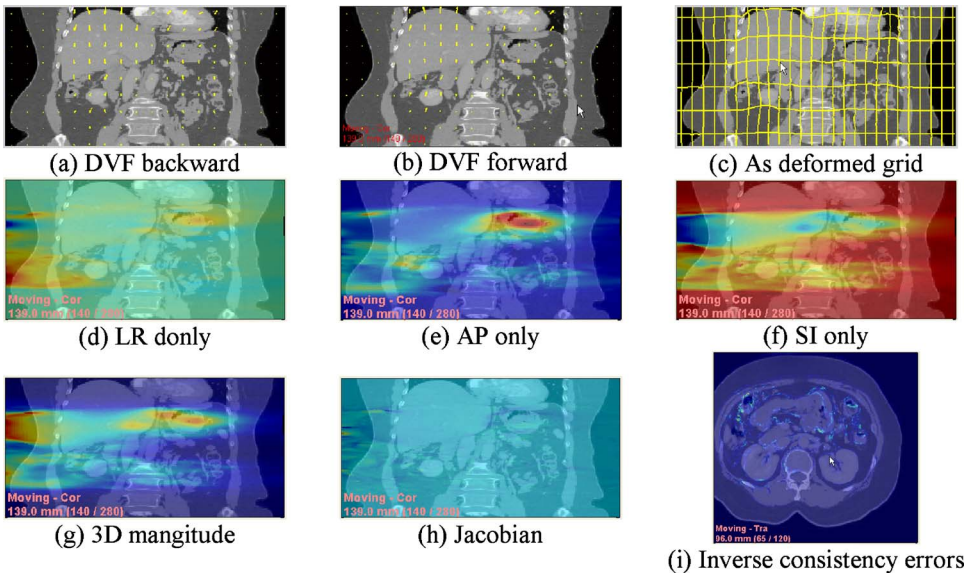

FIG. 5. DIRART has different ways to display the DVF for user to indirectly evaluate the DIR accuracy. (d)–(i) use different color maps on the purpose of demonstrating the DVF visualization options.

method, which is to automatically extract image features (points, lines, and surfaces) and use these features for validating the DIR results. Useful results and any new DIR verification methods will be added into DIRART in the future.

II.G.2. Evaluation of the DIR results

DIRART offers a few different ways for users to indirectly evaluate the DIR results, as shown in Fig. 5.

(1) Visually checking the DVF, as shown in Figs. 5(a)–5(g).
(2) Jacobian analysis.[46] DIRART computes Jacobian values on the DVF to measure contract/expansion, as shown in Fig. 5(h), so indirectly gives users a sense of DVF accuracy. Generally, DVF will be certainly problematic where the Jacobian value is less than 0.5, or greater than 1.5.
(3) Inverse consistency analysis.[33] DIRART can compute the inverse consistency errors for DVF computed in forward and backward registration direction. Inverse consistency errors, as shown in Fig. 5(i), could give the lower bound the absolute registration errors.

III. RESULTS

We use the data from a head-and-neck cancer patient to demonstrate how DIRART might be used. This patient was initially treated with IMRT for the left side with the initial CT scan. After a few months, this patient was retreated with IMRT on the right side with a new CT scan and a new set of structure contours. In this example, the researcher desires to consider the first and finished treatment in the optimization of the second IMRT plan. To evaluate the second IMRT plan, the target coverage requirements and dosimetric constraints on all critical OARs should be evaluated on the total dose (by both treatments) that the patient to receive, instead of only the second plan dose.

Because the first IMRT plan was done on the different CT scans, there is currently no simple way to warp the first plan dose onto the second CT scan for the second IMRT plan to be optimized with the initial condition. DIRART, however, could provide help in this situation.

Figure 6 shows a screenshot of the DIRART GUI to demonstrate some of the DIRART visualization options. There are seven display panels used in this example. Each panel is individually configured to display different or combined data, in different 3D views, zooming settings, color setting, etc. There are two plan doses that are displayed in isodose lines (with or without labels) and with different color wash and color map options. Structures could be displayed with only contour lines or with color filled. DVF could be displayed as vectors or as deformed grid lines. Line colors and thickness are configurable. The difference images could be shown in either colors or in grayscales.

Figure 7 shows how the deformable image registration is carried out. The first CT scan [Fig. 7(a)] is used as the moving image for DIR. The second CT scan [Fig. 7(b)] is used as the fixed image. Both images are visually aligned. One can see some tissue deformation between the two CT scans from the grayscale difference image in Fig. 7(c). Figure 7(d) is the difference between the deformed (registered) first CT scan and the second CT scan. It shows that the tissue alignment is visually improved. The deformation vectors shown in Fig. 7(d) give sense about how tissue deforms.

Figure 7 also shows the structure contours along with the images. Figure 7(c), the difference image before registration, shows that structures from different plans are generally misaligned slightly. After DIR, the structures from one plan could be remapped onto the CT scan of the other plan, which is demonstrated in Fig. 7(d). One can see that the remapped spinal cord matches better to the secondary spinal cord in Fig. 7(d). Remapped structures from one CT scan onto the other CT scan could be useful to evaluate the dose distributions. They can also be useful to indirectly evaluate the ac-

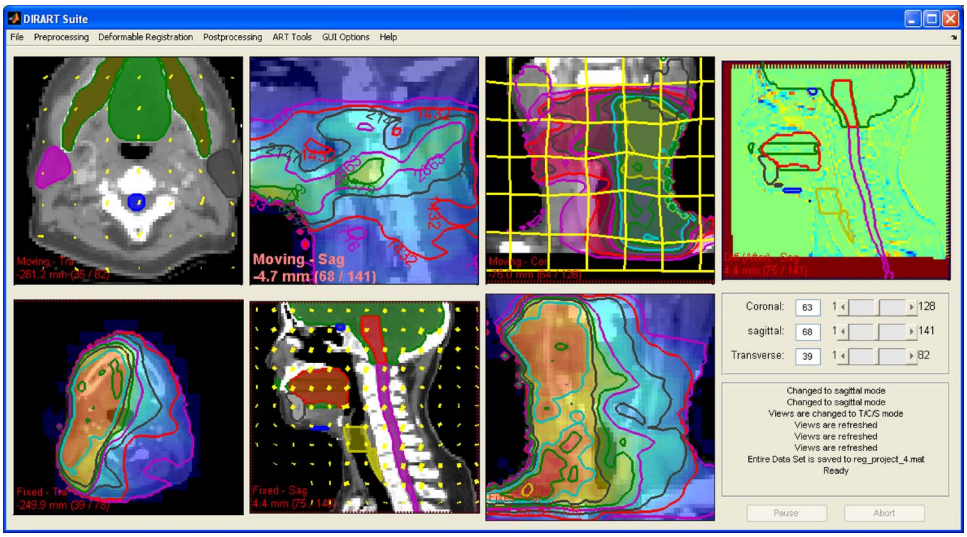

FIG. 6. A screenshot of the DIRART main GUI to demonstrate the visualization features. Color bars, which are not shown, can be turned on from the GUI option menu.

curacy of DIR, assuming the remapped structures should match well with the structures manually drawn on the other CT scan. Structure remapping from one scan to the secondary scan is also a general way of autosegmentation if the secondary scan is not contoured and DIR is accurate enough.

Figure 8 shows the examples to remap the first dose distribution onto the second CT scan so that both dose distributions can be summed up on the second CT scan. The final dose sum is useful to compute the composite DVHs to evaluate the second IMRT plan.

IV. DISCUSSION

IV.A. Performance and computation speed

We have found the computation time of the DIR algorithms in DIRART to be acceptable for research purposes. This is partly due to the fact that research activities are not as demanding as clinical work in terms of speed and partly due to the fact that DIRART functions can be accessed and executed via scripts. Those who desire more speed can easily crop images or change the voxel resolution using basic

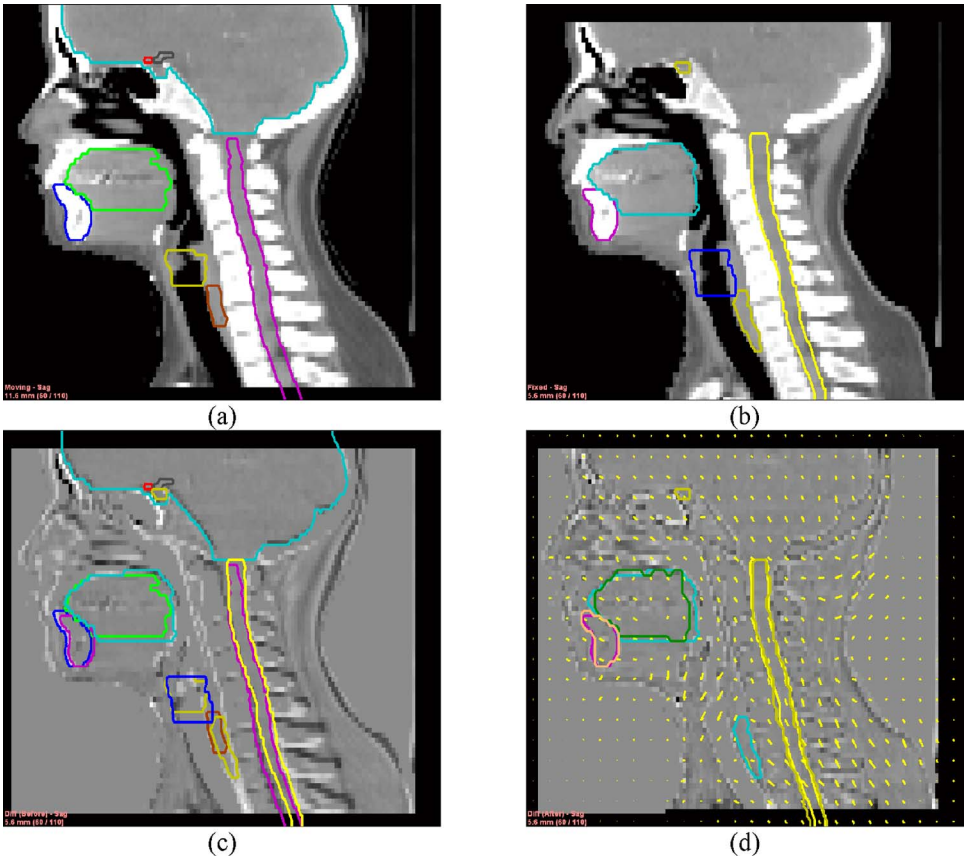

FIG. 7. Demonstration of deformable image registration and structure contour remapping on the H/N cancer patient. (a) The initial CT scan with the initial structure contours. (b) The second CT scan with the secondary structure contours. (c) The different images before deformable image registration with both sets of structure contours. (d) The different images after image registration overlaid with deformation vectors, with the remapped initial structure contours and the secondary structure contours.

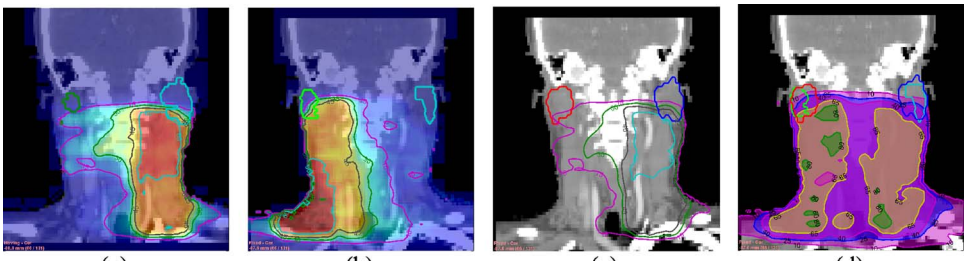

FIG. 8. Demonstration of dose deformation and accumulation. (a) Dose of the initial plan overlaid on the first CT scan with the contours of both parotids. (b) Dose of the second plan overlaid on the second CT scan with the both parotids (contoured on the second scan). (c) The deformed initial dose on the second CT scan with the initial parotid contours remapped onto the second CT scans. (d) The sum of doses of both plans on the second CT scan with both the remapped initial parotid contours and the secondary parotid contours. Different color map schemes are used in (c) and (d) to show varieties of the dose visualization options in DIRART.

DIRART functions. For example, we used a $2\times2\times3$ mm^3 resolution for the head-and-neck patient example in Sec. III. For image sizes of $130\times140\times82$, the DIR computation finishes in 80 s on a Dell Optiplex 755 desktop PC with 2.66 GHz CPU and 2 GB RAM. This time will vary as a function of the DIR voxel resolution, the size of the images, and the values of the DIR computation parameters. There are plans to further improve the computation speed using GPU approaches in the near future.

IV.B. Distribution

The authors have made DIRART an open-source project, hosted on Google at http://dirart.googlecode.com. DIRART is free to use for research proposes. Any contributor to DIRART should follow the open-source copyright rules and is therefore responsible for their code. Complete user instructions and other documentations are available from the same URL. The project has become too large in scale for authors alone to further maintain and improve it. The authors hope that DIRART will benefit from mass collaboration in the same manner as CERR and other open-source projects have. The open-source nature of the effort should allow other people to easily contribute to the project, allow users to easily access the latest bug fixes and major updates, and allow users to beta test the new features, to report bugs, and to comment on the new changes.

IV.C. Versus ITK/VTK/MITK

ITK/VTK/MITK are much larger software toolkits than DIRART. They are not only for radiation oncology but for the entire image-processing community. DIRART is more focused on medical imaging, radiation oncology, and ART, and could be more natural to start with for users from these focused fields. GUI of DIRART is generally slower than VTK or MITK because of MATLAB versus C++/OPENGL. ITK has more DIR algorithms implemented, but DIRART provides a few important and unique features that are not available in ITK or other academic DIR implementations (inverse consistency, NaN image patching, etc.). It is worth to emphasize again that DIRART supports a number of ITK algorithms in the current version and will certainly support more ITK DIR algorithms available in the near future.

IV.D. Based on MATLAB

MATLAB is a widely adopted scientific research platform. It provides not only a very rich set of functions for scientific computation but also a relative easy program language to create applications with essential graphics presentations. MATLAB is an excellent data handling tool, is cross platform, supports very readable coding, and is easily extensible by users. In addition, CERR is based on MATLAB and produces easily manipulable MATLAB RT objects. Many radiotherapy researchers are familiar with the MATLAB/CERR combination. The CERR import/export routines have been widely tested on data from virtually every commercial treatment planning system. Also, MATLAB has very good programming toolboxes. Other high-level program languages, like C/C++, are better programming languages for performance sensitive applications. For example, ITK is fully programed in C/C++. However, the coding style of ITK itself does not emphasize efficiency. The DIR applications in DIRART have been implemented in MATLAB code. Interestingly, the DIR algorithms implemented in DIRART in MATLAB have similar computation performance as the comparable DIR algorithms from ITK. Overall, the implementation of DIRART in MATLAB seems to be efficient for research applications, and there is still a room to further improve the performance.

IV.E. Limitations

DIRART does not have a dose computation engine to compute daily doses from daily images and treatment plans. However, this could be compensated by using the dose computation engine with CERR. DIRART also does not do online or offline adaptive treatment planning reoptimization based on daily images, which is a completely different topic.

IV.F. Future work

Our future plan for DIRART includes (1) integrate more ITK DIR algorithms into DIRART, especially spline-based algorithms and FEM algorithms, (2) computation speed improve-

ment via GPU acceleration, (3) be able to exchange DVF objects with other ART software tools, and (4) add a simple work flow manager to allow scripting multiple steps of ART data processing.

V. CONCLUSION

DIRART is a software suite for deformable image registration and adaptive radiotherapy research. With the integrated GUI, it provides a friendly environment to the users to perform DIR and ART tasks without having to be overwhelmed by the details of DIR algorithms and ART operations. In addition, it fills the need of such robust and open-source software tools in the radiotherapy field and has great potential in its roles as an ART research environment and a DIR research and development software suite. Finally, as an open-source project, DIRART can be upgraded for future research needs.

ACKNOWLEDGMENTS

This research was partially supported by the NIH (Grant No. CA118200) and a grant from Tomotherapy, Inc.

[a]Electronic mail: dyang@radonc.wustl.edu

[1]D. Yan *et al.*, "Adaptive radiation therapy," Phys. Med. Biol. **42**, 123–132 (1997).
[2]J. O. Deasy *et al.*, "CERR: A computational environment for radiotherapy research," Med. Phys. **30**, 979–985 (2003).
[3]T. R. Mackie *et al.*, "Image guidance for precise conformal radiotherapy," Int. J. Radiat. Oncol., Biol., Phys. **56**, 89–105 (2003).
[4]D. A. Jaffray *et al.*, "Flat-panel cone-beam computed tomography for image-guided radiation therapy," Int. J. Radiat. Oncol., Biol., Phys. **53**, 1337–49 (2002).
[5]L. A. Dawson *et al.*, "Advances in image-guided radiation therapy," J. Clin. Oncol. **25**, 938–946 (2007).
[6]T. S. Hong *et al.* "The impact of daily setup variations on head-and-neck intensity-modulated radiation therapy," Int. J. Radiat. Oncol., Biol., Phys. **61**, 779–788 (2005).
[7]M. A. Hawkins *et al.*, "Assessment of residual error in liver position using kV cone-beam computed tomography for liver cancer high-precision radiation therapy," Int. J. Radiat. Oncol., Biol., Phys. **66**, 610–619 (2006).
[8]E. K. Hansen *et al.*, "Repeat CT imaging and replanning during the course of IMRT for head-and-neck cancer," Int. J. Radiat. Oncol., Biol., Phys. **64**, 355–362 (2006).
[9]J. L. Barker *et al.*, "Quantification of volumetric and geometric changes occurring during fractionated radiotherapy for head-and-neck cancer using an integrated CT/linear accelerator system," Int. J. Radiat. Oncol., Biol., Phys. **59**, 960–970 (2004).
[10]C. E. Noel *et al.*, "An automated method for adaptive radiation therapy for prostate cancer patients using continuous fiducial-based tracking," Phys. Med. Biol. **55**, 65–82 (2010).
[11]J. Chen *et al.*, "Dose-guided radiation therapy with megavoltage cone-beam CT," Br. J. Radiol. **79**, S87–S98 (2006).
[12]J. D. Chapman *et al.* "Molecular (functional) imaging for radiotherapy applications: An RTOG symposium," Int. J. Radiat. Oncol., Biol., Phys. **55**, 294–301 (2003).
[13]P. M. Price *et al.*, "The role of PET scanning in radiotherapy," Br. J. Radiol. **S28**, 2–4 (2005).
[14]D. Yang *et al.*, "Deformable registration of abdominal kilovoltage treatment planning CT and tomotherapy daily megavoltage CT for treatment adaptation," Med. Phys. **36**, 329–338 (2009).
[15]K. K. Brock *et al.*, "Feasibility of a novel deformable image registration technique to facilitate classification, targeting, and monitoring of tumor and normal tissue," Int. J. Radiat. Oncol., Biol., Phys. **64**, 1245–1254 (2006).
[16]S. S. Samant *et al.*, "High performance computing for deformable image registration: Towards a new paradigm in adaptive radiotherapy," Med. Phys. **35**, 3546–3553 (2008).
[17]X. Han *et al.*, "Atlas-based auto-segmentation of head and neck CT Images," in *Proceedings of the 11th International Conference on Medical Image Computing and Computer-Assisted Intervention, Part II* (Springer-Verlag, New York, 2008).
[18]B. Haas *et al.*, "Automatic segmentation of thoracic and pelvic CT images for radiotherapy planning using implicit anatomic knowledge and organ-specific segmentation strategies," Phys. Med. Biol. **53**, 1751–1771 (2008).
[19]G. Olivera *et al.*, "Image guided radiotherapy plan evaluation based on deformable dose registration from daily on-line positioning images," Int. J. Radiat. Oncol., Biol., Phys. **63**, S508–S509 (2005).
[20]J. Orban de Xivry *et al.*, "Tumour delineation and cumulative dose computation in radiotherapy based on deformable registration of respiratory correlated CT images of lung cancer patients," Radiother. Oncol. **85**, 232–238 (2007).
[21]Q. Wu *et al.*, "Application of dose compensation in image-guided radiotherapy of prostate cancer," Phys. Med. Biol. **51**, 1405–1419 (2006).
[22]G. J. Price *et al.*, "A method to calculate coverage probability from uncertainties in radiotherapy via a statistical shape model," Phys. Med. Biol. **52**, 1947–1965 (2007).
[23]G. X. Ding *et al.*, "A study on adaptive IMRT treatment planning using kV cone-beam CT," Radiother. Oncol. **85**, 116–125 (2007).
[24]C. Wu *et al.*, "Re-optimization in adaptive radiotherapy," Phys. Med. Biol. **47**, 3181–3195 (2002).
[25]Q. J. Wu *et al.*, "On-line re-optimization of prostate IMRT plans for adaptive radiation therapy," Phys. Med. Biol. **53**, 673–691 (2008).
[26]Insight Segmentation and Registration Toolkit (www.itk.org).
[27]W. Schroeder *et al.*, *Visualization Toolkit: An Object-Oriented Approach to 3D Graphics*, 4th ed. (Kitware, Clifton Park, NY, 2006).
[28]D. Maleike *et al.*, "Interactive segmentation framework of the medical imaging interaction toolkit," Comput. Methods Programs Biomed. **96**, 72–83 (2009).
[29]A. Buades *et al.*, "A review of image denoising algorithms, with a new one," Multiscale Model. Simul. **4**, 490–530 (2005).
[30]K. Zuiderveld, *Graphics Gems IV* (Academic, New York, 1994), pp. 474–485.
[31]D. Yang *et al.*, "Technical Note: Deformable image registration on partially matched images for radiotherapy applications," Med. Phys. **37**(1), 141–145 (2010).
[32]J. B. Maintz *et al.*, "A survey of medical image registration," Med. Image Anal. **2**, 1–36 (1998).
[33]D. Yang *et al.*, "A fast inverse consistent deformable image registration method based on symmetric optical flow computation," Phys. Med. Biol. **53**, 6143–6165 (2008).
[34]B. C. Vemuri *et al.*, "Image registration via level-set motion: Applications to atlas-based segmentation," Med. Image Anal. **7**, 1–20 (2003).
[35]S. L. Iu *et al.*, "Re-examining the optical flow constraint. A new optical flow algorithm with outlier rejection," presented at the International Conference on Image Processing, 1999 (unpublished).
[36]P. J. Burt *et al.*, "The Laplacian pyramid as a compact image code," IEEE Trans. Commun. **31**, 532–540 (1983).
[37]J. P. Thirion, "Image matching as a diffusion process: An analogy with Maxwell's demons," Med. Image Anal. **2**, 243–260 (1998).
[38]B. K. P. Horn *et al.*, "Determining optical flow," Artif. Intell. **17**, 185–203 (1981).
[39]B. D. Lucas *et al.*, "An iterative image registration technique with an application to stereo vision," Proceedings of the Seventh International Joint Conference on Artificial Intelligence, pp. 674–679, 1981 (unpublished).
[40]A. Bruhn *et al.*, "Lucas/Kanade meets Horn/Schunck: Combining local and global optic flow methods," Int. J. Comput. Vis. **61**(3), 211–231 (2005).
[41]J. L. Barron *et al.*, "Performance of optical flow techniques," Int. J. Comput. Vis. **12**, 43–77 (1994).
[42]W. Lu *et al.*, "Fast free-form deformable registration via calculus of variations," Phys. Med. Biol. **49**, 3067–3087 (2004).
[43]H. Wang *et al.*, "Validation of an accelerated 'demons' algorithm for deformable image registration in radiation therapy," Phys. Med. Biol. **50**, 2887–2905 (2005).

[44]P. Rogelj *et al.*, "Symmetric image registration," Med. Image Anal. **10**, 484–493 (2006).
[45]B. C. Vemuri *et al.*, "A level-set based approach to image registration," presented at the Proceedings of the IEEE Workshop on Mathematical Methods in Biomedical Image Analysis, Hilton Head Island, SC, 2000 (unpublished).
[46]A. Leow *et al.*, "Inverse consistent mapping in 3D deformable image registration: Its construction and statistical properties," *Information Processing in Medical Imaging* (Springer, Berlin, 2005), Vol. 3565, pp. 493–503.